J. Appl. Comput. Mech., 4(3) (2018) 202-215
DOI: 10.22055/jacm.2017.23096.1149

ISSN: 2383-4536
jacm.scu.ac.ir

Shahid Chamran University of Ahvaz

Journal of Applied and Computational Mechanics

Research Article

Semi-Analytical Solution for Vibration of Nonlocal Piezoelectric Kirchhoff Plates Resting on Viscoelastic Foundation

D.P. Zhang[1], Y.J. Lei[2], Z.B. Shen[3]

[1] College of Aerospace Science and Engineering, National University of Defense Technology, Changsha, Hunan 410073, China

Received August 22 2017; Revised September 26 2017; Accepted for publication October 01 2017.
Corresponding author: Yongjun Lei, leiyj108@nudt.edu.cn
Copyright © 2018 Shahid Chamran University of Ahvaz. All rights reserved.

Abstract. Semi-analytical solutions for vibration analysis of nonlocal piezoelectric Kirchhoff plates resting on viscoelastic foundation with arbitrary boundary conditions are derived by developing Galerkin strip distributed transfer function method. Based on the nonlocal elasticity theory for piezoelectric materials and Hamilton's principle, the governing equations of motion and boundary conditions are first obtained, where external electric voltage, viscoelastic foundation, piezoelectric effect, and nonlocal effect are considered simultaneously. Subsequently, Galerkin strip distributed transfer function method is developed to solve the governing equations for the semi-analytical solutions of natural frequencies. Numerical results from the model are also presented to show the effects of nonlocal parameter, external electric voltages, boundary conditions, viscoelastic foundation, and geometric dimensions on vibration responses of the plate. The results demonstrate the efficiency of the proposed methods for vibration analysis of nonlocal piezoelectric Kirchhoff plates resting on viscoelastic foundation.

Keywords: Nonlocal piezoelectric plates; Vibration characteristics; Viscoelastic foundation; Galerkin strip distributed transfer function method.

1. Introduction

Plate and plate-like structures play a crucial role in many areas of mechanical, civil, and aerospace engineering. As a result, numerous studies have been performed by researchers to examine the static deflection, vibration, buckling, and wave propagation of plates based on classical plate models in the last century. Recently, piezoelectric plates have attracted considerable attention from science and engineering communities due to their exceptional electro-mechanical coupling effect [1,2]. This novel property makes piezoelectric plates promising for the building blocks of actuators, mass and pressure sensors, acceleration sensors, and etc. It is thus important to have a better understanding of the mechanical properties and other physical properties of piezoelectric plates from theoretical and engineering points of view. Although the vibration of piezoelectric nanoplates has been studied a lot in recent years, little study on the vibration of piezoelectric macroplates has been reported. On the other hand, in the analysis of dynamic properties, the macroplates are often idealized as classical Kirchhoff plate models and classical Mindlin plate models.

However, the nonlocal elasticity theory established by Eringen [3,4] points out that the stress at a reference point is affected not only by the strain at that point but also by the strains at every point in the domain. Owing to the consideration of nonlocal effect, the nonlocal elasticity theory has been widely used in the research of nanostructures, such as carbon nanotubes (CNTs), boron nanotubes (BNNTs), and graphene (GS) [5-8]. Actually, the nonlocal effect exists not only in the mechanical properties of nanostructures but also in those of macrostructures. Hache et al. [9] argued that: "A basic approach to justify the use of nonlocal models is to consider whether the structure is represented by discrete systems that are composed of finite number of cells." Obviously, as the dimensions of the structure are close to those of its cells, the nonlocal effect becomes increasingly important, and the discrete structure can no longer be homogenized into the continuum.

On this basis, the nonlocal elasticity theories have been employed to study the mechanical properties of macrostructures. Hache et al. [9] studied both stability and vibration of nonlocal beams and plates subjected to compressive forces, where various nonlocal structural models were developed for lattice-based beams and plates. A nonlocal damped Kirchhoff plate model was proposed by Lei et al. [10] to examine the dynamic responses of plates in macroscale based on Galerkin method and the nonlocal elasticity theory. Also, a nonlocal viscoelastic foundation model was developed by Lei [11] to analyze the vibration of beams in macroscale with various boundary conditions based on the nonlocal elasticity theory. Zhao et al. [12] investigated the strain responses for a nonlocal viscoelastic Kelvin bar in tension, where the strain fields in closed form were obtained by transforming governing equations into Volterra integration form. Friswell et al. [13] developed a nonlocal viscoelastic beam model to study the dynamics behavior of beams with various boundary conditions by using the finite element method. In the above studies, the nonlocal effect on the dynamic responses of macrostructures has been investigated preliminarily.

Moreover, the nonlocal elasticity theories have been widely used in dynamic responses of nanostructures. Based on the nonlocal Kirchhoff plate theory and Pasternak-type elastic foundation model, Asemi and Farajpour [14] investigated the thermo-electro-mechanical vibration for a coupled piezoelectric-nanoplate system which was embedded in an elastic medium and subjected to a non-uniform voltage distribution. A nonlocal Kirchhoff plate theory was also developed by Asemi et al. [15] to investigate the effect of initial stress on the vibration responses of double-piezoelectric-nanoplate systems, where the Pasternak-type elastic foundation model was employed to consider the effect of shearing between the two nanoplates. Based on the visco-nonlocal-piezoelasticity theories, Kolahchi et al. [16] examined the dynamic stability of piezoelectric nanoplates embedded in a viscoelastic medium. The visco-nonlocal-refined Zigzag theories were applied by Kolahchi et al. [17] to investigate the dynamic buckling of sandwich nanoplates subjected to harmonic compressive loads. Arefi and Zenkour [18] examined the free vibration of a sandwich nanoplate resting on visco-Pasternak's foundation based on the nonlocal Kirchhoff theory and Hamilton's principle. A nonlocal quasi-3D theory was developed by Bouafia et al. [19] to study the bending and free flexural vibration of functionally graded (FG) nanobeams. Based on the nonlocal zeroth-order shear deformation theory, Bounouara et al. [20] investigated the free vibration of FG nanoplates resting on an elastic foundation. The nonlocal zeroth-order shear deformation theory was also applied by Bellifa et al. [21] to examine the nonlinear post-buckling behavior of nanobeams. In this study, the closed-form solutions for the critical buckling load and the amplitude of the static nonlinear response in the post-buckling state were derived. Chaht et al. [22] studied the bending and buckling behaviors of nanobeams made of functionally graded materials (FGMs) including the thickness stretchiness effect by using nonlocal continuum model. A nonlocal trigonometric shear deformation theory was developed by Besseghier et al. [23] to investigate the free vibration analysis of FG nanoplates resting on two-parameter elastic foundation. The nonlocal trigonometric shear deformation theory was also used by Ahouel et al. [24] to analyze the bending, buckling, and vibration of FG nanobeams. Based on the nonlocal first-order shear deformation theory, Bedia et al. [25] studied the thermal buckling characteristics of armchair SWCNTs embedded in an elastic medium. In the research, a closed-form solution for non-dimensional critical buckling temperature was also obtained. Belkorissat et al. [26] proposed a new nonlocal hyperbolic refined plate model to examine the free vibration properties of FG nanoplates.

To the best of the present authors' knowledge, the vibration of nonlocal piezoelectric Kirchhoff plates in macroscale has not been reported in the literature when a viscoelastic foundation is considered. The information, however, is extremely important for the modern engineering applications of piezoelectric plates. As a result, the present paper is devoted to examining the vibration of nonlocal piezoelectric Kirchhoff plates resting on a viscoelastic foundation, as shown in Fig. 1. The governing equations of motion and boundary conditions are first derived by using Hamilton's principle. The Galerkin strip distributed transfer function method is then developed to derive the semi-analytical solutions for the natural frequencies of nonlocal piezoelectric Kirchhoff plates with arbitrary boundary conditions. The proposed model is validated by comparing the obtained results with those available in the literature. The effects of nonlocal parameter, external electric voltages, boundary conditions, viscoelastic foundation, and geometric dimensions on the vibration characteristics of the plate are also carefully discussed.

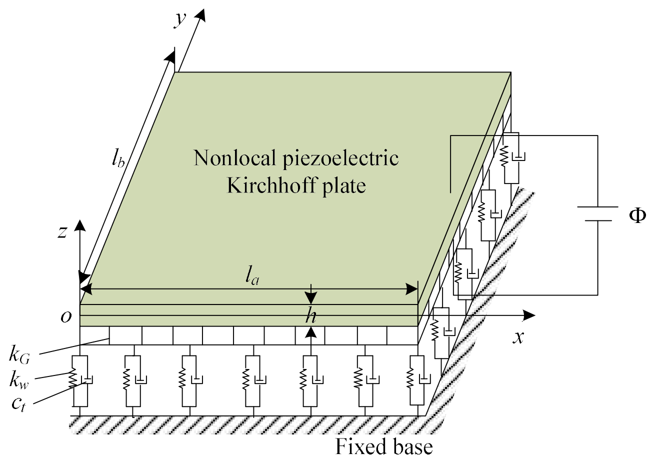

Fig. 1. Schematic configuration of a nonlocal piezoelectric Kirchhoff plate resting on viscoelastic foundation

2. Governing equations of motion for vibration analysis

In this section, the governing equations of motion and boundary conditions for vibration analysis of nonlocal piezoelectric Kirchhoff plates resting on a viscoelastic foundation are derived based on the nonlocal elasticity theory. As shown in Fig. 1, let us consider a nonlocal piezoelectric Kirchhoff plate with length l_a, width l_b and thickness h resting on a visco-Pasternak foundation. Based on the nonlocal elasticity theory for piezoelectric materials [1, 27, 28], the basic equations for the plate can be expressed as:

$$\left(1-(e_0 a)^2\nabla^2\right)\sigma_{ij} = c_{ijkl}\varepsilon_{kl} - e_{ijk}E_k \tag{1}$$

$$\left(1-(e_0 a)^2\nabla^2\right)D_I = e_{ikl}\varepsilon_{kl} - k_{ik}E_k \tag{2}$$

$$\sigma_{ij,j} = \rho\ddot{u}_i,\ D_{i,j} = 0,\ E_i = -\Phi_i \tag{3}$$

where σ_{ij} is nonlocal stress, ε_{kl} is nonlocal strain, D_i is electric displacement, E_k is electric field vector, and u_i is displacement vector. Moreover, the terms c_{ijkl}, e_{ijk}, κ_{ik}, and ρ are the elastic constants, piezoelectric constants, dielectric constants, and mass density of the plate, respectively. Based on the Kirchhoff plate theory, the displacement components in the x-, y-, and z-directions can be written as:

$$\begin{aligned}
u_1(x,y,z,t) &= u(x,y,t) - z\frac{\partial w(x,y,t)}{\partial x},\\
u_2(x,y,z,t) &= v(x,y,t) - z\frac{\partial w(x,y,t)}{\partial y},\\
u_3(x,y,z,t) &= w(x,y,t).
\end{aligned} \tag{4}$$

where $u(x, y, t)$, $v(x, y, t)$, and $w(x, y, t)$ denote the mid-plane displacement components. In addition to the displacement fields, the electric potential distribution for the plate should also be defined. Following Quek and Wang [29], the electric potential distribution $\Phi(x, y, z, t)$ is assumed as a combination of cosine and linear variation as follows:

$$\Phi(x,y,z,t) = -\cos\left(\frac{\pi z}{h}\right)\phi(x,y,t) + \frac{2zV_0}{h} \tag{5}$$

where $\Phi(x, y, t)$ and V_0 are the electric potential in the mid-plane and external electric voltage, respectively. By substituting Eq. (5) into Eq. (3), the electric field can be obtained as:

$$E_x = \cos\left(\frac{\pi z}{h}\right)\frac{\partial\phi}{\partial x}, E_y = \cos\left(\frac{\pi z}{h}\right)\frac{\partial\phi}{\partial y}, E_z - \frac{\pi}{h}\sin\left(\frac{\pi z}{h}\right)\phi - \frac{2V_0}{h}. \tag{6}$$

Moreover, according to Eq. (4), the strain-displacement equations for the plate can also be written as:

$$\varepsilon_{xx} = \frac{\partial u}{\partial x} - z\frac{\partial^2 w}{\partial x^2}, \varepsilon_{yy} = \frac{\partial v}{\partial y} - z\frac{\partial^2 w}{\partial y^2}, \gamma_{xy} = \frac{\partial u}{\partial y} + \frac{\partial v}{\partial x} - 2z\frac{\partial^2 w}{\partial x\partial y}, \varepsilon_{xz} = \varepsilon_{yz} = \varepsilon_{zz} = 0. \tag{7}$$

The strain energy Π_S of the nonlocal piezoelectric Kirchhoff plate can be calculated from:

$$\begin{aligned}
\Pi_S &= \frac{1}{2}\int_A\int_{-h/2}^{h/2}(\sigma_{xx}\varepsilon_{xx} + 2\sigma_{xy}\varepsilon_{xy} + \sigma_{yy}\varepsilon_{yy} - D_x E_x - D_y E_y - D_z E_z)dzdA\\
\Pi_S &= \frac{1}{2}\int_A \rho h\left[(\frac{\partial u}{\partial t})^2 + (\frac{\partial v}{\partial t})^2 + (\frac{\partial w}{\partial t})^2\right]dA\\
&-\frac{1}{2}\int_A\int_{-h/2}^{h/2}\left[D_x\cos\left(\frac{\pi z}{h}\right)\frac{\partial\phi}{\partial x} + D_y\cos\left(\frac{\pi z}{h}\right)\frac{\partial\phi}{\partial y} - D_z\left(\frac{\pi}{h}\sin\left(\frac{\pi z}{h}\right)\phi + \frac{2V_0}{h}\right)\right]dzdA
\end{aligned} \tag{8}$$

where A is the area of the mid-plane, $\{N_{xx}, N_{yy}, N_{xy}\}$ and $\{M_{xx}, M_{yy}, M_{xy}\}$ are the stress resultants and stress couples, respectively, which can be expressed as:

$$\{N_{xx}, N_{yy}, N_{xy}\} = \int_{-h/2}^{h/2}\{\sigma_{xx}, \sigma_{yy}, \sigma_{xy}\}dz \tag{9}$$

$$\{M_{xx}, M_{yy}, M_{xy}\} = \int_{-h/2}^{h/2}\{\sigma_{xx}, \sigma_{yy}, \sigma_{xy}\}zdz \tag{10}$$

In addition, the kinetic energy Π_k and external work Π_F are respectively given by:

$$\Pi_k = \frac{1}{2}\int_A \rho h\left[(\frac{\partial u}{\partial t})^2 + (\frac{\partial v}{\partial t})^2 + (\frac{\partial w}{\partial t})^2\right]dA \tag{11}$$

$$\Pi_k = \frac{1}{2}\int_A \rho h\left[-N_Q w + N_{Ex}(\frac{\partial w}{\partial x})^2 + N_{Ey}(\frac{\partial w}{\partial y})^2\right]dA \tag{12}$$

where N_Q is the reaction of the viscoelastic foundation, N_{Ex} and N_{Ey} are the normal forces induced by external electric voltage V_0 in the x- and y- directions. Furthermore, we have:

$$N_Q = k_w w - k_G \nabla^2 w + c_t \frac{\partial w}{\partial t} \tag{13}$$

$$N_{Ex} = N_{Ey} = -2\tilde{e}_{31} V_0 \tag{14}$$

where k_w, k_G, and c_t are used to denote the Winkler's modulus parameter, Pasternak's modulus parameter, and damping parameter, respectively. Based on the nonlocal Kirchhoff plate theory, the basic equations for the plate presented as Eqs. (1) and (2) can be rewritten as:

$$\begin{aligned}
&\left(1-(e_0a)^2\nabla^2\right)\sigma_{xx} = \tilde{c}_{11}\varepsilon_{xx} + \tilde{c}_{12}\varepsilon_{yy} - \tilde{e}_{31}E_z\,,\\
&\left(1-(e_0a)^2\nabla^2\right)\sigma_{yy} = \tilde{c}_{12}\varepsilon_{xx} + \tilde{c}_{11}\varepsilon_{yy} - \tilde{e}_{31}E_z\,,\\
&\left(1-(e_0a)^2\nabla^2\right)\sigma_{xy} = \tilde{c}_{66}\gamma_{xy}\,,
\end{aligned} \tag{15}$$

$$\begin{aligned}
&\left(1-(e_0a)^2\nabla^2\right)D_x = \tilde{k}_{11}E_x\,,\\
&\left(1-(e_0a)^2\nabla^2\right)D_y = \tilde{k}_{11}E_y\,,\\
&\left(1-(e_0a)^2\nabla^2\right)D_z = \tilde{e}_{31}\varepsilon_{xx} + \tilde{e}_{31}\varepsilon_{yy} + \tilde{k}_{33}E_z\,,
\end{aligned} \tag{16}$$

where:

$$\tilde{c}_{11} = c_{11} - \frac{c_{13}^2}{c_{33}}, \tilde{c}_{12} = c_{12} - \frac{c_{13}^2}{c_{33}}, \tilde{c}_{66} = c_{66}, \tilde{e}_{31} = e_{31} - \frac{c_{13}e_{33}}{c_{33}}, \tilde{k}_{11} = k_{33} + \frac{e_{33}^2}{c_{33}}. \tag{17}$$

Consider the Hamilton's principle:

$$\int_0^t (\delta\Pi_k + \delta\Pi_F - \delta\Pi_S)dt = 0 \tag{18}$$

We can derive the governing equations of motion as follows:

$$\begin{aligned}
\delta w:\ &\frac{\partial^2 M_{xx}}{\partial x^2} + 2\frac{\partial^2 M_{xy}}{\partial x \partial y} + \frac{\partial^2 M_{yy}}{\partial y^2} - \left(k_w w - k_G \nabla^2 w + c_t \frac{\partial w}{\partial t}\right)\\
&- N_{Ex}\frac{\partial^2 w}{\partial x^2} - N_{Ey}\frac{\partial^2 w}{\partial y^2} = \rho h \frac{\partial^2 w}{\partial t^2}
\end{aligned} \tag{19}$$

$$\delta\phi: \int_{-h/2}^{h/2}\left[\frac{\partial D_x}{\partial x}\cos\left(\frac{\pi z}{h}\right) + \frac{\partial D_y}{\partial y}\cos\left(\frac{\pi z}{h}\right) + D_z\frac{\pi}{h}\sin\left(\frac{\pi z}{h}\right)\right]dz = 0 \tag{20}$$

and the corresponding boundary conditions:

$$w = 0, or\left[\frac{\partial M_{xx}}{\partial x} + \frac{\partial M_{xy}}{\partial y} - N_{Ex}\frac{\partial w}{\partial x}\right]n_x + \left[\frac{\partial M_{xy}}{\partial x} + \frac{\partial M_{yy}}{\partial y} - N_{Ey}\frac{\partial w}{\partial y}\right]n_y = 0 \tag{21}$$

$$\frac{\partial w}{\partial x} = 0, or, M_{xx}n_x + M_{xy}n_y = 0 \tag{21}$$

$$\frac{\partial w}{\partial x} = 0, or, M_{xx}n_x + M_{xy}n_y = 0 \tag{22}$$

$$\frac{\partial w}{\partial x} = 0, or, M_{xy}n_x + M_{yy}n_y = 0 \tag{23}$$

$$\phi = 0, or\int_{-h/2}^{h/2}\left[\cos\left(\frac{\pi z}{h}\right)D_x n_x + \cos\left(\frac{\pi z}{h}\right)D_y n_y\right]dz = 0 \tag{24}$$

Here, (n_x, n_y) are the direction cosines of the outward unit normal to the boundaries of the mid-plane. According to Eqs. (7), (10), (15) and (16), the governing Eqs. (19) and (20) can be written as:

$$\begin{aligned}
&-d_{11}\frac{\partial^4 \overline{w}}{\partial \xi^4} - 2(d_{12}+2d_{66})\lambda^2\frac{\partial^4 \overline{w}}{\partial \xi^2 \partial \xi^2} - d_{11}\lambda^4\frac{\partial^4 \overline{w}}{\partial \xi^4} + \overline{F}_{31}\eta^2\left(\frac{\partial^2}{\partial \xi^2} + \lambda^2\frac{\partial^2}{\partial \xi^2}\right)\overline{\phi}\\
&-\left[1-\alpha^2\left(\frac{\partial^2}{\partial \xi^2} + \lambda^2\frac{\partial^2}{\partial \xi^2}\right)\right]\left[\begin{array}{l}\overline{k}_w\eta^2\overline{w} - \overline{k}_G\eta^2\left(\frac{\partial^2}{\partial \xi^2} + \lambda^2\frac{\partial^2}{\partial \xi^2}\right)\overline{w} + \overline{c}_t\eta^2\frac{\partial \overline{w}}{\partial t}\\ +\overline{N}_{Ex}\eta^2\frac{\partial^2 \overline{w}}{\partial \xi^2} + \overline{N}_{Ey}\eta^2\lambda^2\frac{\partial^2 \overline{w}}{\partial \xi^2}\end{array}\right] = \left[1-\alpha^2\left(\frac{\partial^2}{\partial \xi^2} + \lambda^2\frac{\partial^2}{\partial \xi^2}\right)\right]\eta^2\frac{\partial^2 \overline{w}}{\partial t^2}
\end{aligned} \tag{25}$$

$$\bar{X}_{11}\frac{\partial^2\bar{\phi}}{\partial\xi^2}+\bar{X}_{11}\lambda^2\frac{\partial^2\bar{\phi}}{\partial\xi^2}-\bar{F}_{31}\frac{\partial^2 w}{\partial\xi^2}-\bar{F}_{31}\frac{\partial^2 w}{\partial\xi^2}-\bar{X}_{33}\eta^2\bar{\phi}=0 \tag{26}$$

$$\{D_{11},D_{12},D_{66}\}=\int_{-h/2}^{h/2}\{\tilde{c}_{11},\tilde{c}_{12},\tilde{c}_{66}\}z^2dz \tag{27}$$

$$F_{31}=\int_{-h/2}^{h/2}\tilde{e}_{31}\frac{\pi}{h}z\sin\left(\frac{\pi z}{h}\right)dz \tag{28}$$

$$X_{11}=\int_{-h/2}^{h/2}\tilde{k}_{11}\cos^2\left(\frac{\pi z}{h}\right)dz, X_{33}=\int_{-h/2}^{h/2}\tilde{k}_{33}\left(\frac{\pi}{h}\right)^2\sin^2\left(\frac{\pi z}{h}\right)dz \tag{29}$$

$$\begin{gathered}\xi=\frac{x}{l_a},\xi=\frac{y}{l_b},\bar{w}=\frac{w}{h},\eta=\frac{l_a}{h},\lambda=\frac{l_a}{l_b},\alpha=\frac{e_0a}{l_a},\bar{c}_{11}=\tilde{c}_{11}h,\phi_0=\sqrt{\bar{c}_{11}/X_{33}},\bar{\phi}=\frac{\phi}{\phi_0},\\ \bar{k}_w=\frac{k_wl_\alpha^2}{\bar{c}_{11}},\bar{k}_G=\frac{k_G}{\bar{c}_{11}},\bar{c}_t=\frac{c_tl_a}{\sqrt{\rho h\bar{c}_{11}}},t=\frac{t}{l_a}\sqrt{\frac{\bar{c}_{11}}{\rho h}},\bar{X}_{11}=\frac{X_{11}\phi^2}{\bar{c}_{11}h^2},\bar{X}_{33}=\frac{X_{33}\phi_0^2}{\bar{c}_{11}},\\ \{\bar{N}_{Ex},\bar{N}_{Ey}\}=\frac{1}{\bar{c}_{11}}\{\bar{N}_{Ex},\bar{N}_{Ey}\}\{d_{11},d_{12},d_{66}\}=\frac{1}{\bar{c}_{11}h^2}\{D_{11},D_{12},D_{66}\},\bar{F}=\frac{F_{31}\phi_0}{\bar{c}_{11}h}\\ \Omega_{mn}=\omega_{mn}l_a\sqrt{\rho h/\bar{c}_{11}}.\end{gathered} \tag{30}$$

It is understood that the exact analytical solutions may not be available for the natural frequencies of nonlocal piezoelectric Kirchhoff plates resting on a viscoelastic foundation. To obtain the semi-analytical solution for the natural frequencies of nonlocal piezoelectric Kirchhoff plates, a new numerical approach called the Galerkin strip distributed transfer function method (GSDTFM) is developed in the next section.

3. GSDTFM for nonlocal piezoelectric Kirchhoff plates

As shown in Fig. 2, the nonlocal piezoelectric Kirchhoff plate is first divided into *NE* strip elements along *x*-axis. The transverse displacement $w(x,y,t)$ and the electric potential $\phi(x,y,t)$ of the *e*-th strip element are defined as:

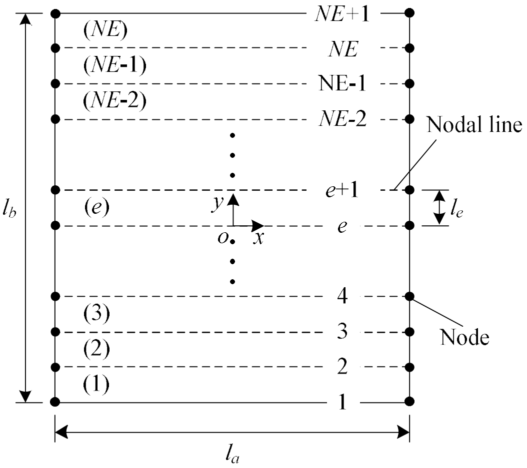

Fig. 2. A rectangular nonlocal piezoelectric Kirchhoff plate dispersed into strips.

$$w(x,y,t)=N(y)\delta_{e,w}(x,t) \tag{31}$$

$$\phi(x,y,t)=N(y)\delta_{e,\phi}(x,t) \tag{32}$$

where vectors $\delta_{e,w}(x,t)$ and $\delta_{e,\phi}(x,t)$ are given as:

$$\delta_{e,w}(x,t)=\left[w_i(x,t),\theta_i(x,t),w_j(x,t),\theta_j(x,t)\right]^T \tag{33}$$

$$\delta_{e,\phi}(x,t)=\left[\phi_i(x,t),\vartheta_i(x,t),\phi_j(x,t),\vartheta_j(x,t)\right]^T \tag{34}$$

and $N(y)$ denotes the matrix of shape functions:

$$N(y)=\left[1-3\frac{y^2}{l^2}+2\frac{y^3}{l^3},y-2\frac{y^2}{l}+\frac{y^3}{l^2},3\frac{y^2}{l^2}-2\frac{y^3}{l^3},-\frac{y^2}{l}+\frac{y^3}{l^2}\right] \tag{35}$$

Here, $\{w_i, w_j\}$, $\{\theta_i, \theta_j\}$, and $\{\phi_i, \phi_j\}$ are the transverse displacements, rotations, and electric potentials on the two nodal lines of the *e*-th strip element, respectively, and $\{\vartheta_i, \vartheta_j\}$ are the first-order partial derivatives of electric potentials $\{\phi_i, \phi_j\}$ with respect to y. According to the dimensionless terms presented as Eq. (30), Eqs. (31)-(34) can be rewritten as:

$$\overline{w}(\zeta,\xi,l)=\overline{N}(\xi)\overline{\delta}_{e,w}(\zeta,l) \tag{36}$$

$$\overline{\phi}(\zeta,\xi,l)=\overline{N}(\xi)\overline{\delta}_{e,\phi}(\zeta,l) \tag{37}$$

$$\overline{N}(\xi)=\left[1-3\frac{\xi^2}{l^2}+2\frac{\xi^3}{l^3},l_b\left(\xi-2\frac{\xi^2}{\overline{l}}+\frac{\xi^3}{l^2}\right),3\frac{\xi^2}{l^2}-2\frac{\xi^3}{l^3},l_b\left(-\frac{\xi^2}{\overline{l}}+\frac{\xi^3}{l^2}\right)\right] \tag{38}$$

$$\overline{\delta}_{e,w}(\zeta,l)=\left[\overline{w}_i,\overline{\theta}_i,\overline{w}_j,\overline{\theta}_j\right]^T \tag{39}$$

$$\overline{\delta}_{e,\phi}(\zeta,l)=\left[\overline{\phi}_i,\overline{\vartheta}_i,\overline{\phi}_j,\overline{\vartheta}_j\right]^T \tag{40}$$

where

$$\left\{\overline{\theta}_i,\overline{\theta}_j\right\}=\frac{1}{h}\left\{\theta_i,\theta_j\right\},\left\{\overline{\vartheta}_i,\overline{\vartheta}_j\right\}=\frac{1}{\phi_0}\left\{\vartheta_i,\vartheta_j\right\},\overline{l}=\frac{l}{l_b} \tag{41}$$

Furthermore, the force boundary conditions at the two nodal lines can be given by:

$$\begin{cases}F_{sy}^t\Big|_{y=0}=-\left(F_{sy}+\dfrac{\partial M_{xy}}{\partial x}\right)\Big|_{y=0}=0\\ M_{yy}\Big|_{y=0}=0\end{cases},\begin{cases}F_{sy}^t\Big|_{y=0}=-\left(F_{sy}+\dfrac{\partial M_{xy}}{\partial x}\right)\Big|_{y=1}=0\\ M_{yy}\Big|_{y=1}=0\end{cases} \tag{42}$$

where F_{sy}^t and $F_{sy}=\partial M_{xy}/\partial x+\partial M_{yy}/\partial y$ are equivalent shear force and shear force, respectively. According to Eqs. (25), (27) and (42), the weak form of Eqs. (25) and (29) can be calculated from:

$$\begin{aligned}&-\int_0^{\overline{l}}\overline{H}\left(d_{11}\frac{\partial^4\overline{w}}{\partial\zeta^4}+d_{12}\lambda^2\frac{\partial^4\overline{w}}{\partial\zeta^2\partial\xi^2}-\overline{F}_{31}\eta^2\frac{\partial^2\overline{\phi}}{\partial\zeta^2}\right)d\xi+\int_0^{\overline{l}}4d_{66}\lambda^2\frac{\partial\overline{H}}{\partial\xi}\frac{\partial^3\overline{w}}{\partial\zeta^2\partial\xi}d\xi\\
&-\int_0^{\overline{l}}\frac{\partial^2\overline{H}}{\partial\xi^2}\left(d_{12}\lambda^2\frac{\partial^2\overline{w}}{\partial\zeta^2}+d_{11}\lambda^4\frac{\partial^2\overline{w}}{\partial\xi^2}-\overline{F}_{31}\eta^2\lambda^2\overline{\phi}\right)d\xi\\
&-\int_0^{\overline{l}}\overline{H}\left[1-\alpha^2\left(\frac{\partial^2}{\partial\zeta}+\lambda^2\frac{\partial^2}{\partial\xi}\right)\right]\left[\overline{k}_w\eta^2\overline{w}-\overline{k}_G\eta^2\left(\frac{\partial^2}{\partial\zeta^2}+\lambda^2\frac{\partial^2}{\partial\xi^2}\right)\overline{w}+\overline{c}_t\eta^2\frac{\partial\overline{w}}{\partial t}\right]d\xi\\
&-\int_0^{\overline{l}}\overline{H}\left[1-\alpha^2\left(\frac{\partial^2}{\partial\zeta^2}+\lambda^2\frac{\partial^2}{\partial\xi^2}\right)\right]\overline{N}_{Ex}\eta^2\frac{\partial^2\overline{w}}{\partial\zeta^2}d\xi\\
&-\int_0^{\overline{l}}\overline{H}\left[1-\alpha^2\left(\frac{\partial^2}{\partial\zeta^2}+\lambda^2\frac{\partial^2}{\partial\xi^2}\right)\right]\overline{N}_{Ey}\eta^2\lambda^2\frac{\partial^2\overline{w}}{\partial\zeta^2}d\xi\\
&-\int_0^{\overline{l}}\overline{H}\left[1-\alpha^2\left(\frac{\partial^2}{\partial\zeta^2}+\lambda^2\frac{\partial^2}{\partial\xi^2}\right)\right]\eta^2\lambda^2\frac{\partial^2\overline{w}}{\partial t^2}d\xi=0\end{aligned} \tag{43}$$

$$\int_0^{\overline{l}}\overline{H}\left(\overline{X}_{11}\frac{\partial^2\overline{\phi}}{\partial\zeta^2}+\overline{X}_{11}\lambda^2\frac{\partial^2\overline{\phi}}{\partial\xi^2}-\overline{X}_{33}\eta^2\overline{\phi}-\overline{F}_{31}\frac{\partial^2\overline{w}}{\partial\zeta^2}-\overline{F}_{31}\lambda^2\frac{\partial^2\overline{w}}{\partial\xi^2}\right)d\xi=0$$

$$\int_0^{\overline{l}}\overline{H}\left(\overline{X}_{11}\frac{\partial^2\overline{\phi}}{\partial\zeta^2}+\overline{X}_{11}\lambda^2\frac{\partial^2\overline{\phi}}{\partial\xi^2}-\overline{X}_{11}\eta^2\overline{\phi}-\overline{F}_{31}\frac{\partial^2\overline{w}}{\partial\zeta^2}-\overline{F}_{31}\lambda^2\frac{\partial^2\overline{w}}{\partial\xi^2}\right)d\xi^2=0 \tag{44}$$

where $\overline{H}$ denotes admissible function. By substituting Eqs. (36) and (37) into Eqs. (43) and (44), and taking $\overline{H}=\overline{N}^T$, we have:

$$\begin{aligned}&\overline{k}_e^{(4)}\frac{\partial^4\overline{\delta}_{e,w}}{\partial\zeta^4}+\overline{k}_e^{(2)}\frac{\partial^2\overline{\delta}_{e,w}}{\partial\zeta^2}+\overline{k}_e^{(0)}\overline{\delta}_{e,w}+\overline{m}_e^{(1)}\frac{\partial\overline{\delta}_{e,w}}{\partial t}+\overline{k}_e^{(2)}\frac{\partial^2\overline{\delta}_{e,w}}{\partial\zeta^2\partial t}+\overline{m}_e^{(2)}\frac{\partial^2\overline{\delta}_{e,w}}{\partial t^2}\\
&+\overline{k}_{e,2}^{(2)}\frac{\partial^4\overline{\delta}_{e,w}}{\partial\zeta^2\partial t^2}+\overline{k}_e^{(2)'}\frac{\partial^2\overline{\delta}_{e,\phi}}{\partial\zeta^2}+\overline{k}_e^{(2)'}\overline{\delta}_{e,\phi}=0\end{aligned} \tag{45}$$

$$\overline{g}_e^{(2)}\frac{\partial^2\overline{\delta}_{e,w}}{\partial\zeta^2}+\overline{g}_e^{(0)}\overline{\delta}_{e,w}+\overline{g}_e^{(2)'}\frac{\partial\overline{\delta}_{e,\phi}}{\partial\zeta^2}+\overline{g}_e^{(0)'}\overline{\delta}_{e,\phi}=0 \tag{46}$$

where $\overline{k}_e^{(4)},\overline{k}_e^{(2)},\overline{k}_e^{(0)},\overline{k}_{e,1}^{(2)},\overline{k}_{e,2}^{(2)},\overline{k}_e^{(2)'},\overline{k}_e^{(0)'},\overline{g}_e^{(2)},\overline{g}_e^{(0)},\overline{g}_e^{(2)'},\overline{g}_e^{(0)'}$ are strip stiffness matrices, and $\overline{m}_e^{(1)},\overline{m}_e^{(2)}$ are strip mass m atrices. The expressions of these matrices are listed in Appendix *A* for easy reference. If we define the global nodal line displacement and electric potential vectors as:

$$\bar{\delta}_w(\zeta,l)=\left[\bar{w}_1,\bar{\theta}_1,\bar{w}_2,\bar{\theta}_2,...\bar{w}_{NE+1},\bar{\theta}_{NE+1}\right]^T \tag{47}$$

$$\bar{\delta}_\phi(\zeta,l)=\left[\bar{\phi}_1,\bar{\vartheta}_1,\bar{\phi}_2,\bar{\vartheta}_2,...\bar{\phi}_{NE+1},\bar{\vartheta}_{NE+1}\right]^T \tag{48}$$

Then, the global dynamic equilibrium equations of nonlocal piezoelectric Kirchhoff plates can be derived as:

$$\begin{aligned}&\bar{K}^{(4)}\frac{\partial^4\bar{\delta}_w}{\partial\zeta^4}+\bar{K}^{(2)}\frac{\partial^4\bar{\delta}_w}{\partial\zeta^2}+\bar{K}^{(0)}\bar{\delta}_w+\bar{M}^{(1)}\frac{\partial\bar{\delta}_w}{\partial t}+\bar{K}_1^{(2)}\frac{\partial^3\bar{\delta}_w}{\partial\zeta^2\partial t}+\bar{M}^{(2)}\frac{\partial^2\bar{\delta}_w}{\partial t^2}\\&\bar{K}_2^{(2)}\frac{\partial^4\bar{\delta}_w}{\partial\zeta^2\partial t^2}+\bar{K}^{(2)\prime}\frac{\partial^4\bar{\delta}_\phi}{\partial\zeta^2}+\bar{K}^{(0)\prime}\bar{\delta}_\phi=0\end{aligned} \tag{49}$$

$$G^{-(2)}\frac{\partial^2\bar{\delta}_w}{\partial\zeta^2}+G^{-(0)}\bar{\delta}_w+G^{-(2)\prime}\frac{\partial^2\bar{\delta}_\phi}{\partial\zeta^2}+G^{-(0)}\bar{\delta}_\phi=0 \tag{50}$$

where $\bar{K}_e^{(4)},\bar{K}_e^{(2)},\bar{K}_e^{(0)},\bar{K}_{e,1}^{(2)},\bar{K}_{e,2}^{(2)},\bar{K}_e^{(2)\prime},\bar{K}_e^{(0)\prime},\bar{G}_e^{(2)},\bar{G}_e^{(0)},\bar{G}_e^{(2)\prime},\bar{G}_e^{(0)\prime}$ are global stiffness matrices, and $\bar{M}_e^{(1)},\bar{M}_e^{(2)}$ are global mass matrices. Assuming that $\bar{\delta}_w$ consists of N_1 unknown nodal line displacements $\bar{\delta}_w'$ and N_2 known nodal line displacements $\bar{\delta}_w''$, we have:

$$\bar{\delta}_w=T_1\bar{\delta}_w'+T_2\bar{\delta}_w' \tag{51}$$

where T_1 and T_2 are row transformation matrices containing 0 and 1. Similarly, the global electric potential vector $\bar{\delta}_\phi$ can be rewritten as:

$$\bar{\delta}_\phi=T_1\bar{\delta}_\phi'+T_2\bar{\delta}_\phi' \tag{52}$$

Substituting Eqs. (51) and (52) into Eqs. (53) and (54) yields:

$$\begin{aligned}&\tilde{k}^{(4)}\frac{\partial^4\bar{\delta}_w'}{\partial\zeta^4}+\tilde{k}^{(2)}\frac{\partial^2\bar{\delta}_w'}{\partial\zeta^2}+\tilde{k}^{(0)}\bar{\delta}_w'+\tilde{M}^{(1)}\frac{\partial\bar{\delta}_w'}{\partial t}+\tilde{k}_1^{(2)}\frac{\partial^3\bar{\delta}_w'}{\partial\zeta^2\partial t}+\tilde{M}^{(2)}\frac{\partial^2\bar{\delta}_w'}{\partial t^2}\\&+\tilde{k}_2^{(2)}\frac{\partial^4\bar{\delta}_w'}{\partial\zeta^2\partial t^2}+\tilde{k}^{(2)\prime}\frac{\partial^2\bar{\delta}_w'}{\partial\zeta^2}+\tilde{k}^{(0)\prime}\bar{\delta}_w'=0\end{aligned} \tag{53}$$

$$\tilde{G}^{(2)}\frac{\partial^2\bar{\delta}_w'}{\partial\zeta^2}+\tilde{G}^{(0)}\bar{\delta}_w'+\tilde{G}^{(2)\prime}\frac{\partial^2\bar{\delta}_\phi'}{\partial\zeta^2}+\tilde{G}^{(0)}\bar{\delta}_\phi'=o \tag{54}$$

$$\begin{aligned}&\tilde{K}^{(4)}=T_1^T\bar{K}^{(4)}T_1,\tilde{K}^{(2)}=T_1^T\bar{K}^{(2)}T,\tilde{K}^{(0)}=T_1^T\bar{K}^{(0)}T,\\&\tilde{K}_1^{(2)}=T_1^T\bar{K}_1^{(2)}T,\tilde{K}_2^{(2)}=T_1^T\bar{K}_2^{(2)}T,\tilde{K}^{(2)\prime}=T_1^T\bar{K}^{(2)\prime}T,\\&\tilde{K}^{(0)\prime}=T_1^T\bar{K}^{(0)}T,\tilde{G}^{(2)}=T_1^T\bar{G}^{(2)}T_1,\tilde{G}^{(0)}=T_1^T\bar{G}^{(0)}T_1,\\&\tilde{G}^{(2)\prime}=T_1^T\bar{G}^{(2)\prime}T_1,\tilde{G}^{(0)\prime}=T_1^T\bar{G}^{(0)\prime}T_1,\\&\tilde{M}^{(1)}=T_1^T\bar{M}^{(1)}T_1,\tilde{M}^{(2)}=T_1^T\bar{M}^{(2)}T_1.\end{aligned} \tag{55}$$

Subsequently, the Laplace transform of Eqs. (53) and (54) can be obtained as:

$$\begin{aligned}&\tilde{K}^{(4)}\frac{\partial^4\hat{\delta}_w}{\partial\zeta^4}+\tilde{K}^{(2)}\frac{\partial^2\hat{\delta}_w}{\partial\zeta^2}+\tilde{K}^{(0)}\hat{\delta}_w+\tilde{M}^{(1)}\hat{\delta}_w\bar{s}+\tilde{K}_1^{(2)}\frac{\partial^2\hat{\delta}_w}{\partial\zeta^2}\bar{s}+\tilde{M}^{(2)}\hat{\delta}_w\bar{s}^2\\&+\tilde{K}_2^{(2)}\frac{\partial^2\hat{\delta}_w}{\partial\zeta^2}\bar{s}^2+\tilde{K}^{(2)\prime}\frac{\partial^2\hat{\delta}_\phi}{\partial\zeta^2}+\tilde{K}^{(0)}\hat{\delta}_\phi=o\end{aligned} \tag{56}$$

$$\tilde{G}^{(2)}\frac{\partial^2\hat{\delta}_w'}{\partial\zeta^2}+\tilde{G}^{(0)}\hat{\delta}_w'+\tilde{G}^{(2)\prime}\frac{\partial^2\hat{\delta}_\phi'}{\partial\zeta^2}+\tilde{G}^{(0)}\hat{\delta}_\phi'=0 \tag{57}$$

Here, the carat "^" and $\bar{s}$ are used to denote Laplace transformation and Laplace transform parameter, respectively. It is understood that the global dynamic equilibrium Eqs. (56) and (57) are two coupled fourth-order ordinary differential equations for the terms $\bar{\delta}_w'$ and $\bar{\delta}_\phi'$, which can be solved directly by employing the transfer function method (TFM). Therefore, we can define the state vector $\eta(\zeta,\bar{s})$ as:

$$\eta(\zeta,\bar{s})=\left[\hat{\delta}_w'^T\ \frac{\partial\hat{\delta}_w'^T}{\partial\zeta}\ \frac{\partial^2\hat{\delta}_w'^T}{\partial\zeta^2}\ \frac{\partial^3\hat{\delta}_w'^T}{\partial\zeta^3}\ \hat{\delta}_\phi'^T\ \frac{\partial\hat{\delta}_\phi'^T}{\partial\zeta}\right]^T \tag{58}$$

Thus, Eqs. (56) and (57) can be rewritten in a matrix form as:

$$\frac{\partial \eta(\zeta,\bar{s})}{\partial \zeta} = F(\bar{s})(\zeta,\bar{s}) \tag{59}$$

where

$$\boldsymbol{F}\left(\bar{s}\right)=\begin{bmatrix} \mathbf{0} & \boldsymbol{I} & \mathbf{0} & \mathbf{0} & \mathbf{0} & \mathbf{0} \\ \mathbf{0} & \mathbf{0} & \boldsymbol{I} & \mathbf{0} & \mathbf{0} & \mathbf{0} \\ \mathbf{0} & \mathbf{0} & \mathbf{0} & \boldsymbol{I} & \mathbf{0} & \mathbf{0} \\ \boldsymbol{f}_1 & \mathbf{0} & \boldsymbol{f}_2 & \mathbf{0} & \boldsymbol{f}_3 & \mathbf{0} \\ \mathbf{0} & \mathbf{0} & \mathbf{0} & \mathbf{0} & \mathbf{0} & \boldsymbol{I} \\ -\boldsymbol{A}_1\tilde{\boldsymbol{G}}^{(0)} & \mathbf{0} & -\boldsymbol{A}_1\tilde{\boldsymbol{G}}^{(2)} & \mathbf{0} & -\boldsymbol{A}_1\tilde{\boldsymbol{G}}^{(0)'} & \mathbf{0} \end{bmatrix} \tag{60}$$

$$\begin{aligned} f_1 &= -A_2(\tilde{K}^{(0)} + \tilde{M}^{(1)}\bar{s} + \tilde{M}^{(2)}\bar{s}^2 - \tilde{K}^{(2)}A_1\tilde{G}^{(0)}, \\ f_2 &= -A_2(\tilde{K}^{(2)} + \tilde{K}_1^{(2)}\bar{s} + \tilde{K}_2^{(2)}\bar{s}^2 - \tilde{K}^{(2)\prime}A_1\tilde{G}^{(2)}), \\ f_3 &= -A_2(\tilde{K}^{(0)\prime} - \tilde{K}_1^{(2)}A_1\tilde{G}^{(0)}), A_1 = (\tilde{G}^{(2)\prime})^{-1}, A_2 = (\tilde{K}^{(4)})^{-1}. \end{aligned} \tag{61}$$

The solution of Eq. (59) can be expressed as:

$$\eta(\zeta,\bar{s}) = e^{F(\bar{s})\zeta}\eta(0,\bar{s}) \tag{62}$$

The boundary condition of the plate can also be expressed in a matrix form:

$$M_b(\bar{s})\eta(-0.5,\bar{s}) + N_b(\bar{s})\eta(0.5,\bar{s}) = 0 \tag{63}$$

where $M_b(\bar{s})$ and $N_b(\bar{s})$ are boundary condition set matrices at the left and right edges of the plates, respectively. Substituting Eq. (62) into Eq. (63) leads to:

$$\left[M_b(\bar{s})e^{-0.5F(\bar{s})} + N(\bar{s})e^{0.5F(\bar{s})}\right]\eta(0,\bar{s}) = 0 \tag{64}$$

By setting $\bar{s} = i\Omega_{mn}$, the dimensionless natural frequency Ω_{mn} can be derived by solving the following transcendental characteristic equation:

$$\det\left[M_b(i\Omega_{mn})e^{-0.5F(i\Omega_{mn})} + N_b(i\Omega_{mn})e^{0.5F(i\Omega_{mn})}\right] = 0 \tag{65}$$

According to Eq. (30), the natural frequency ω_{mn} of the nonlocal piezoelectric Kirchhoff plate can be calculated from:

$$\omega_{mn} = \frac{\Omega_{mn}}{l_a}\sqrt{\frac{\bar{c}_{11}}{\rho h}} \tag{66}$$

4. Numerical results and discussion

In this section, we present the numerical results for vibration analysis of nonlocal piezoelectric Kirchhoff plates resting on a visco-Pasternak foundation with various boundary conditions (e.g., SSSS, CCSS, and CCCC). The plate is made of PZT-4 with the electric-mechanical material properties presented in Table 1 [30]. Unless otherwise stated, we take the length of the nanoplate l_a=40mm, width l_b=60mm, and thickness h=5mm.

Table 1. Electric-mechanical material properties of PZT-4

c_{11}/GPa	c_{12}/GPa	c_{13}/GPa	c_{33}/GPa	c_{66}/GPa	e_{31}/(C/m^2)
132	71	73	115	30.5	-4.1
e_{15}/(C/m^2)	e_{33}/(C/m^2)	κ_{11}/(C/Vm)	κ_{33}/(C/Vm)	ρ/(kg/m^3)	e_{15}/(C/m^2)
10.5	14.1	5.841×10^{-9}	7.124×10^{-9}	7500	10.5

Table 2 presents the first three dimensionless natural frequencies of nonlocal piezoelectric Kirchhoff plates with varying strip element number NE (here we take α=0.2, $k_w = k_G = c_t = 0$, and V_0= 0). In addition, the analytic solutions of natural frequencies for SSSS piezoelectric nanoplates adopted from Ref. [1] are listed in Table 2. From the table we can see that the natural frequencies of the plate with different boundary conditions are convergent at NE=6. Moreover, it can be observed that the six-strip GSDTFM solutions of the first three dimensionless natural frequencies for SSSS plates are in excellent agreement with those in Ref. [1]. Hence, the six-strip GSDTFM can be used in all of the following numerical calculations.

Table 3 shows the dimensionless fundamental frequencies for SSSS piezoelectric nanoplates with various nonlocal parameters α in comparison with those of Ref. [1]. In Ref. [1], Liu et al. obtained the analytical solution of natural frequencies for the free standing SSSS piezoelectric nanoplate subjected to thermo-electro-mechanical loadings. The parameters applied in this second calculation are the same as those for the above case except that the length of the nanoplate l_a=50nm, width l_b=50nm, and thickness h=5nm. It can be seen from the table that the GSDTFM solutions of the dimensionless fundamental frequencies for SSSS nanoplates in this paper are in excellent agreement with those in the paper [1], which demonstrates the accuracy and efficiency of the proposed method for vibration analysis.

Table 2. The first three dimensionless natural frequencies of nonlocal piezoelectric Kirchhoff plates with varying strip element number *NE*

NE	SSSS			CCSS			CCCC		
	ω_1	ω_2	ω_3	ω_1	ω_2	ω_3	ω_1	ω_2	ω_3
2	0.4532	0.7832	1.0498	0.6125	0.9607	1.2590	0.8089	1.2059	1.4817
3	0.4531	0.7564	1.0498	0.6116	0.9069	1.2576	0.8076	1.0796	1.4791
4	0.4531	0.7542	1.0498	0.6114	0.9032	1.2571	0.8074	1.0757	1.4540
5	0.4531	0.7536	1.0498	0.6114	0.9025	1.2570	0.8072	1.0747	1.4479
6	0.4531	0.7531	1.0498	0.6114	0.9025	1.2569	0.8072	1.0747	1.4479
Ref. [1]	0.4531	0.7531	1.0498	/	/	/	/	/	/

Table 3. The dimensionless fundamental frequencies for SSSS nanoplates in comparison with those of Ref. [1]

A	0.0	0.1	0.2	0.3	0.4	0.5
Present	0.6290	0.5748	0.4702	0.3775	0.3085	0.2582
Ref. [1]	0.6290	0.5748	0.4702	0.3775	0.3085	0.2582

Table 4 shows the first three dimensionless natural frequencies of nonlocal piezoelectric Kirchhoff plates without foundations (i.e., k_w=k_G=c_t=0) and with viscoelastic foundations (k_w=10GPa/n, k_G=0.25Pa·m, and c_t=10-4GPa·s/m) under various boundary conditions. It can be seen from the table that the natural frequencies of plates with various boundary conditions decrease significantly with rising the nonlocal parameter. As the visco-Pasternak foundation is considered, imaginary parts which are related to damping ratios appear in the complex natural frequencies of the plate. The reason for this is that the damping effect of the foundation is introduced into the system. In addition, it can be observed that boundary conditions have strong influence on the real parts of natural frequencies, but have no effect on the imaginary parts. Also, the imaginary parts are not affected by nonlocal parameters. This is because the imaginary parts are only related to the damping of the foundation in which the nonlocal effect is not considered.

Table 4. The first three dimensionless natural frequencies of nonlocal piezoelectric Kirchhoff plates with various boundary conditions and nonlocal parameters α

BCs	Plates without foundations			Plates with visco-Pasternak foundation		
	α=0.0	α=0.1	α=0.2	α=0.0	α=0.1	α=0.2
	0.5678	0.5312	0.4531	0.5995+0.0158i	0.5650+0.0158i	0.4923+0.0158i
SSSS	1.0905	0.9661	0.7531	1.1074+0.0158i	0.9851+0.0158i	0.7774+0.0158i
	1.7423	1.4526	1.0498	1.7529+0.0158i	1.4653+0.0158i	1.0673+0.0158i
	0.7852	0.7286	0.6117	0.8084+0.0158i	0.7537+0.0158i	0.6413+0.0158i
CCSS	1.3377	1.1741	0.9026	1.3515+0.0158i	1.1897+0.0158i	0.9229+0.0158i
	2.1383	1.7616	1.2569	2.1470+0.0158i	1.7721+0.0158i	1.2730+0.0158i
	1.0512	0.9709	0.8151	1.0687+0.0158i	0.9899+0.0158i	0.8306+0.0158i
CCCC	1.6225	1.4134	1.0747	1.6339+0.0158i	1.4265+0.0158i	1.0921+0.0158i
	2.5773	2.0847	1.4491	2.5845+0.0158i	2.0936+0.0158i	1.4618+0.0158i

Fig. 3 to Fig. 8 plot the effect of the nonlocal parameter α on the real parts of the first two nonlocal frequency ratios (NFRs) for nonlocal piezoelectric Kirchhoff plates with various boundary conditions and electric voltage V_0 (here we take k_w=10GPa/n, k_G=0.25Pa·m, and c_t=10-4GPa·s/m). NFR is defined as ω_{NL}/ω_L, where ω_{NL} and ω_L denote the natural frequencies of the nonlocal and classical systems, respectively. Obviously, the first two NFRs for the plate with various boundary conditions and electric voltage V_0 decrease significantly as the nonlocal parameter α increases. This implies that the nonlocal parameter has a strong influence on the vibration characteristics of piezoelectric plates. The possible reason for this is that the rigidity of the plate is reduced due to enhanced nonlocal effect. In addition, such an effect of nonlocal parameter turns out to be more substantial with an increase in both electric voltage V_0 and frequency modes. The significant effect of boundary conditions on NFRs can also be observed in the figures. As the softer constrains are imposed on the boundaries, the effect of nonlocal parameter on the natural frequencies becomes less pronounced.

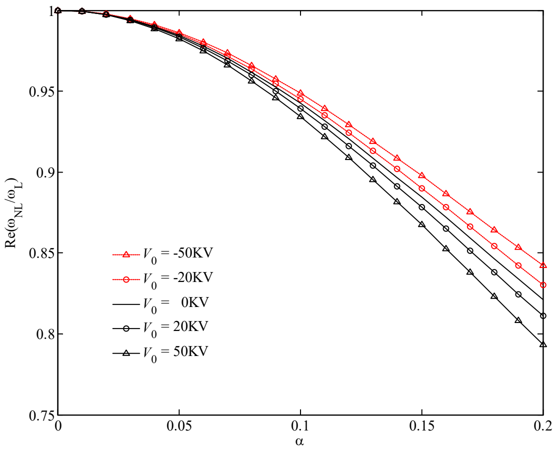

Fig. 3. Effect of nonlocal parameter α on the real parts of the first NFRs for SSSS plates with various electric voltage V_0

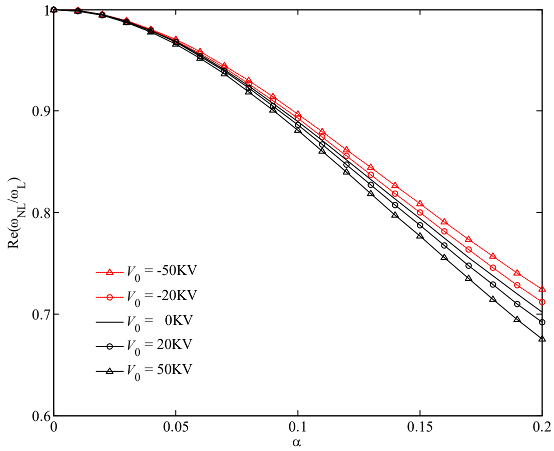

Fig. 4. Effect of nonlocal parameter α on the real parts of the second NFRs for SSSS plates with various electric voltage V_0

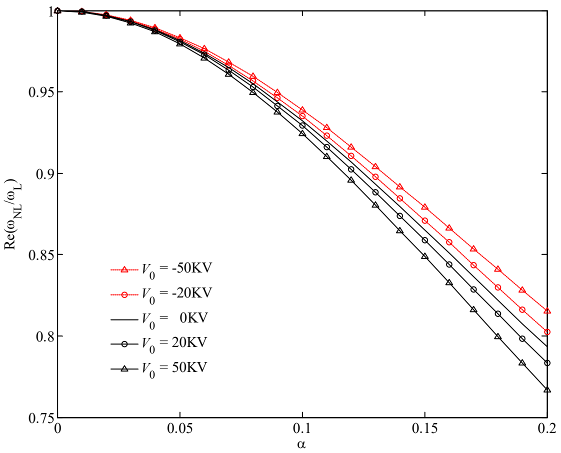

Fig. 5. Effect of nonlocal parameter α on the real parts of the first NFRs for CCSS plates with various electric voltage V_0

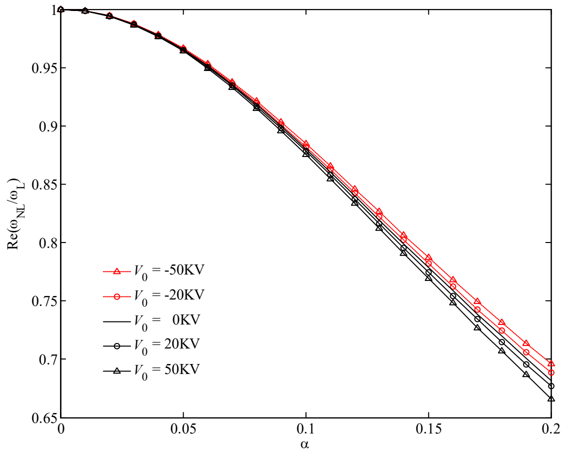

Fig. 6. Effect of nonlocal parameter α on the real parts of the second NFRs for CCSS plates with various electric voltage V_0

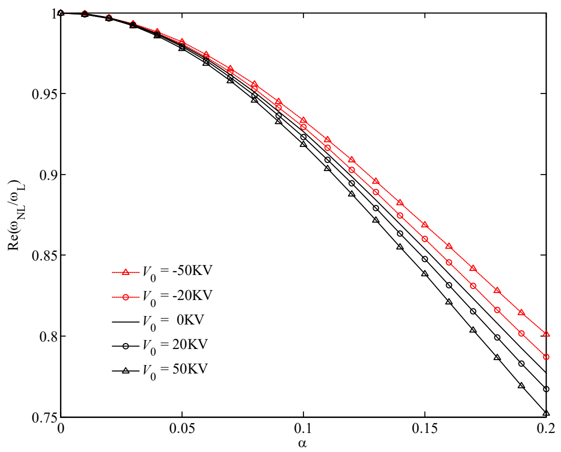

Fig. 7. Effect of nonlocal parameter α on the real parts of the first NFRs for CCCC plates with various electric voltage V_0

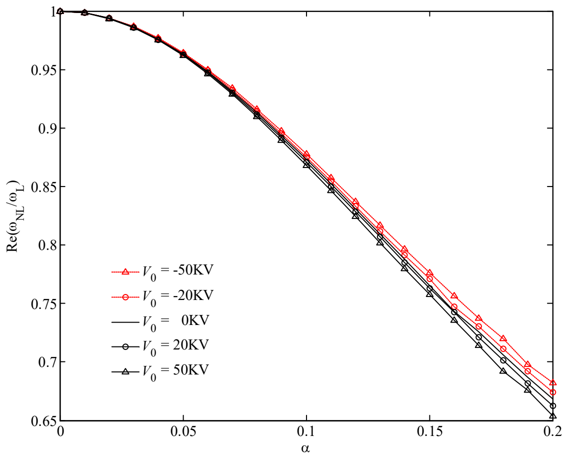

Fig. 8. Effect of nonlocal parameter α on the real parts of the second NFRs for CCCC plates with various electric voltage V_0

Next, we examine the effect of electric voltage V_0 on the real parts of the first two dimensionless natural frequencies for nonlocal piezoelectric Kirchhoff plates with various boundary conditions and the nonlocal parameter α, as shown in Figs. 9-14. In this case, the length of the plate is taken as l_a=40mm, but the width l_b and the thickness h change to satisfy different λ and η. It can be observed from the figures that the first two dimensionless natural frequencies for plates with various boundary conditions decrease almost linearly by raising the electric voltage V_0. This is because the compressive and tensile forces, which will in turn reduce and enhance the stiffness of the plate, will be generated by applying positive and negative external electric voltages, respectively. Furthermore, the effect of external electric voltage V_0 on the natural frequencies turns out to be more substantial as the nonlocal parameter α and the length-to-thickness ratio η increase or the aspect ratio λ decreases. For example, as V_0 increases from -50KV to 50KV, the first dimensionless natural frequencies of SSSS plates decrease about 0.03 with α=0, η=5, and λ=1; about 0.0396 with α=0.2, η=5, and λ=1; about 0.0847 with α=0.2, η=10, and λ=1; and about 0.1469 with α=0.2, η=5, and λ=0.5. On the other hand, we can see that the natural frequencies of the plate decrease significantly with an increase in the length-to-thickness ratio η or a decrease in the aspect ratio λ. The reason for this is that the stiffness of the plate is reduced by increasing the length-to-thickness ratio η or decreasing the aspect ratio λ.

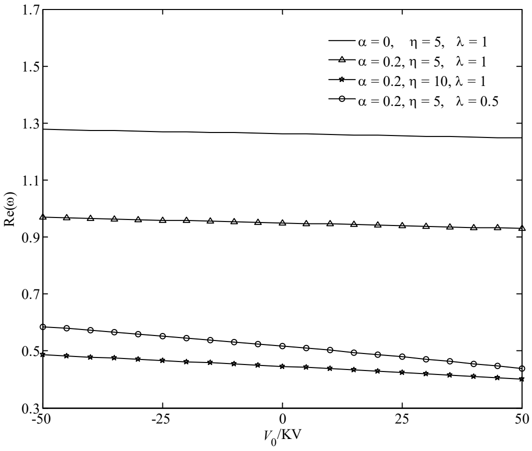

Fig. 9. Effect of electric voltage V_0 on the real parts of the first dimensionless natural frequencies for SSSS plates

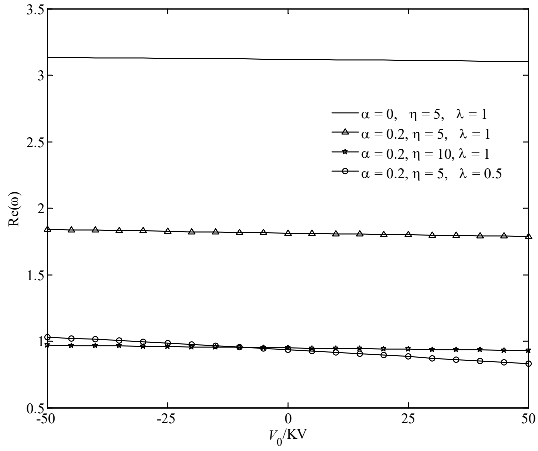

Fig. 10. Effect of electric voltage V_0 on the real parts of the second dimensionless natural frequencies for SSSS plates

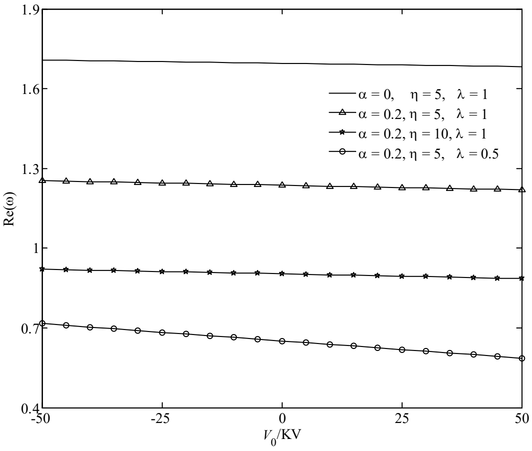

Fig. 11. Effect of electric voltage V_0 on the real parts of the first dimensionless natural frequencies for CCSS plates

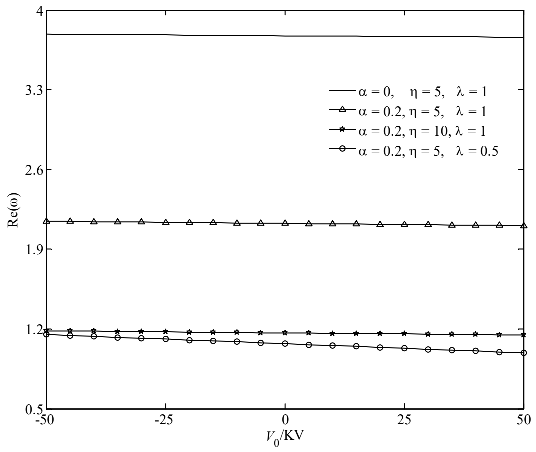

Fig. 12. Effect of electric voltage V_0 on the real parts of the second dimensionless natural frequencies for CCSS plates

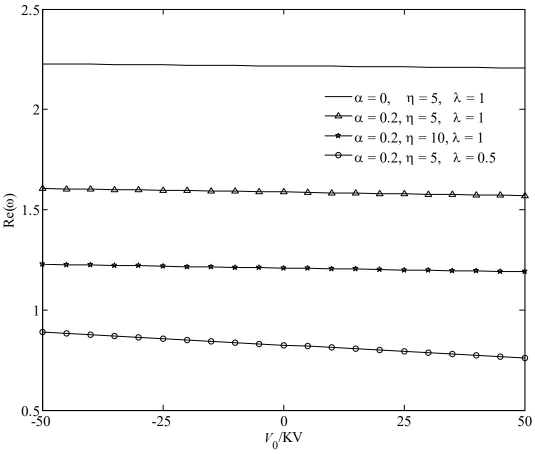

Fig. 13. Effect of electric voltage V_0 on the real parts of the first dimensionless natural frequencies for CCCC plates

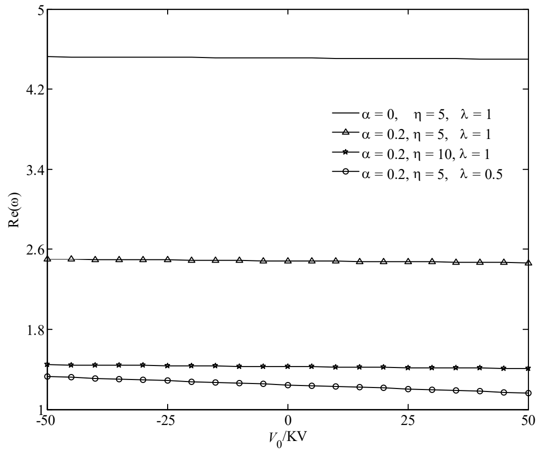

Fig. 14. Effect of electric voltage V_0 on the real parts of the second dimensionless natural frequencies for CCCC plates

As the final numerical example, the variations of the first two complex natural frequencies versus the damping parameter c_t with various Winkler's modulus parameter k_w and the nonlocal parameter α are presented in Figs 15 and 16. From the figures we can see that the real parts of the first two natural frequencies decrease nonlinearly by raising the damping parameter c_t but increase significantly with Winkler's modulus parameter k_w. Furthermore, the real parts remain zero as the damping parameter c_t is larger than a certain value, which is denoted by $(c_t)_{crit}$ to represent the critical value of c_t for non-oscillatory eigen-frequencies. Accordingly, a sharp change can also be seen in the imaginary parts of the first two natural frequencies. In addition, the increase in both mode numbers and Winkler's modulus parameter k_w causes a significant increase in the value of $(c_t)_{crit}$.

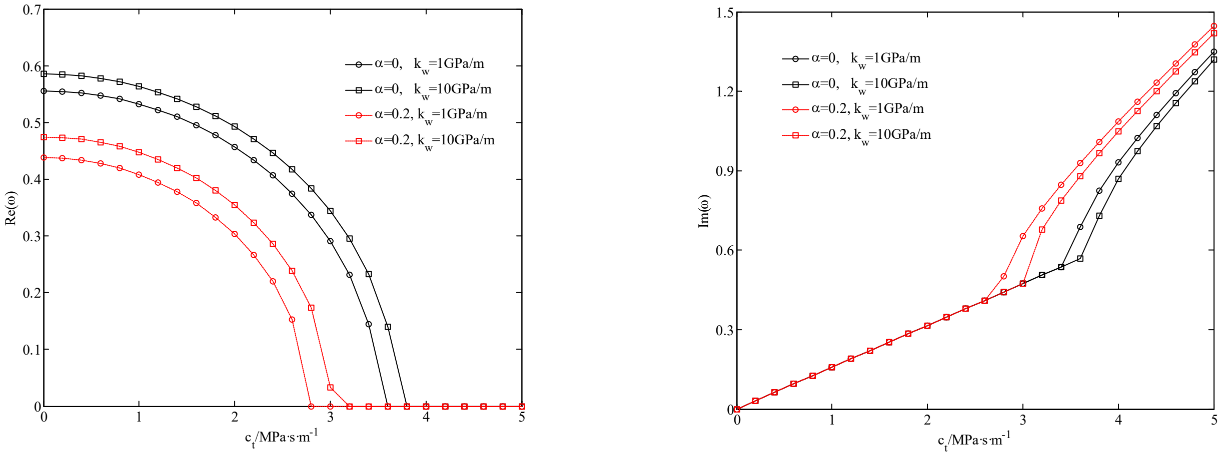

(a) The real parts of natural frequencies (b) The imaginary parts of natural frequencies

Fig. 15. The variation of the first complex dimensionless natural frequencies for SSSS plates with damping parameter c_t

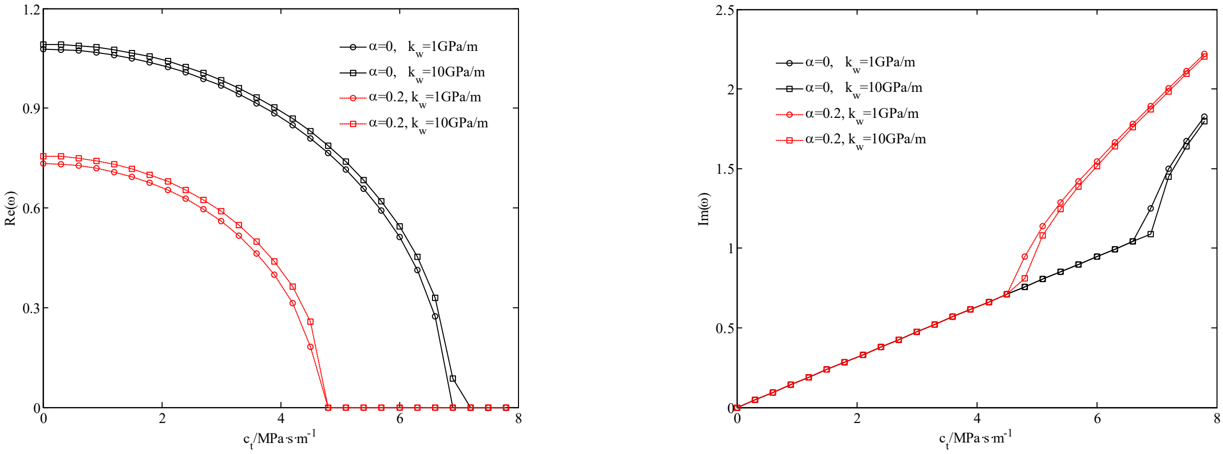

(a) The real parts of natural frequencies (b) The imaginary parts of natural frequencies

Fig. 16. The variation of the second complex dimensionless natural frequencies for SSSS plates with damping parameter c_t

5. Conclusion

The semi-analytical solutions for vibration analysis of nonlocal piezoelectric Kirchhoff plates resting on a viscoelastic foundation with arbitrary boundary conditions are derived by developing the GSDTFM. The governing equations of motion and boundary conditions are first obtained based on the nonlocal elasticity theory and Hamilton's principle. The proposed model is validated by comparing the obtained results with those available in the literature. Subsequently, the effects of nonlocal parameter, external electric voltages, boundary conditions, viscoelastic foundation, and geometric dimensions on the vibration characteristics of the plate are carefully investigated. The results indicate that the natural frequencies of nanoplates decrease significantly by raising the nonlocal parameter. Such an effect of nonlocal parameter becomes more substantial with an increase in both external electric voltage and frequency modes. The natural frequencies of plates with various boundary conditions decrease almost linearly by raising the external electric voltage. The effect of external electric voltage turns out to be more substantial as the nonlocal parameter α and the length-to-thickness ratio η increase or the aspect ratio λ decreases. The damped frequencies of the plate remain zero as the damping parameter c_t of the foundation is larger than $(c_t)_{crit}$, which increases significantly by raising Winkler's modulus parameter kw and mode numbers.

As shown above, the proposed model in this paper can be translated into the classical piezoelectric Kirchhoff plate model by setting the nonlocal parameter to zero and the nonlocal elastic plate model by neglecting the piezoelectric effect. Furthermore, GSDTFM proposed in the present paper, which is combined with the advantages of the traditional strip distributed transfer function method, is available for vibration analysis of the nanoplates not only with arbitrary boundary conditions, but also with arbitrary geometrical shapes.

Acknowledgment

This research is supported by the National Natural Science Foundation of China (Grant Nos. 11272348 and 11302254).

Appendix A

The expressions of strip stiffness matrices and strip mass matrices as appeared in Eqs. (45) and (46) are as follows:

$$\overline{k}_e^{(4)} = -\left[d_{11} + \alpha \overline{k}_G \eta^2 \overline{N}_{Ex}\right] \int_0^{\overline{l}} \overline{N}^T \overline{N} d\xi \tag{A1}$$

$$\begin{aligned} \overline{k}_e^{(2)} &= -\left[d_{12}\lambda^2 + 2\alpha^2 \overline{k}_G \eta^2 \lambda^2 - \alpha^2 \eta^2 \lambda^2 \overline{N}_{Ey} - \alpha^2 \eta^2 \lambda^2 \overline{N}_{Ex}\right] \int_0^{\overline{l}} \overline{N}^T \frac{\partial^2 \overline{N}}{\partial \xi^2} d\xi \\ &+ 4 d_{66} \lambda^2 \int_0^{\overline{l}} \frac{\overline{N}^T}{\partial \xi} \frac{\partial^2 \overline{N}}{\partial \xi} d\xi + \left[\overline{k}_G - \overline{N}_{Ex} + \alpha^2 \overline{k}_w\right] \eta^2 \int_0^{\overline{l}} \overline{N}^T \overline{N} d\xi - d_{12}\lambda^2 \int_0^{\overline{l}} \frac{\partial^2 \overline{N}^T}{\partial \xi^2} \overline{N} d\xi \end{aligned} \tag{A2}$$

$$\overline{k}_{e,2}^{(2)} = \alpha^2 \eta^2 \int_0^{\overline{l}} \overline{N}^T \overline{N} d\xi \tag{A3}$$

$$\overline{k}_{e,1}^{(2)} = \alpha^2 \overline{c}_t \eta^2 \int_0^{\overline{l}} \overline{N}^T \overline{N} d\xi \tag{A4}$$

$$\overline{k}_{e,1}^{(2)} = \overline{F}_{31} \eta^2 \int_0^{\overline{l}} \overline{N}^T \overline{N} d\xi \tag{A5}$$

$$\begin{aligned} \overline{k}_e^{(0)} &= \left[\overline{k}_G - \overline{N}_{Ey} + \alpha^2 \overline{k}_w\right] \eta^2 \lambda^2 \int_0^{\overline{l}} \overline{N}^T \frac{\partial^2 \overline{N}}{\partial \xi^2} d\xi - \overline{k}_w \eta^2 \int_0^{\overline{l}} \overline{N}^T \overline{N} d\xi \\ &+ \left[-\overline{k}_G + \overline{N}_{Ey}\right] \alpha^2 \eta^2 \lambda^4 \int_0^{\overline{l}} \overline{N}^T \frac{\partial^4 \overline{N}}{\partial \xi^4} d\xi - d_{11}\lambda^4 \int_0^{\overline{l}} \frac{\partial^2 \overline{N}^T}{\partial \xi^2} \frac{\partial^2 \overline{N}}{\partial \xi^2} d\xi \end{aligned} \tag{A6}$$

$$\overline{k}_e^{(0)} = \overline{F}_{31} \eta^2 \lambda^2 \int_0^{\overline{l}} \frac{\partial^2 \overline{N}^T}{\partial \xi^2} \overline{N} d\xi \tag{A7}$$

$$\overline{m}_e^{(1)} = \overline{c}_t \eta^2 \int_0^{\overline{l}} \overline{N}^T \overline{N} d\xi + \alpha^2 \overline{c}_t \eta^2 \lambda^2 \int_0^{\overline{l}} \overline{N}^T \frac{\partial^2 \overline{N}}{\partial \xi^2} d\xi \tag{A8}$$

$$\overline{m}_e^{(2)} = -{}_t \eta^2 \int_0^{\overline{l}} \overline{N}^T \overline{N} d\xi + \alpha^2 \eta^2 \lambda^2 \int_0^{\overline{l}} \overline{N}^T \frac{\partial^2 \overline{N}}{\partial \xi^2} d\xi \tag{A9}$$

$$\overline{g}_e^{(2)} = -\overline{F}_{31} \int_0^{\overline{l}} \overline{N}^T \overline{N} d\xi \tag{A10}$$

$$\overline{g}_e^{(2)\prime} = \overline{X}_{11} \int_0^{\overline{l}} \overline{N}^T \overline{N} d\xi \tag{A11}$$

$$\overline{g}_e^{(2)\prime} = \overline{X}_{11} \int_0^{\overline{l}} \overline{N}^T \overline{N} d\xi \tag{A12}$$

$$\overline{g}_e^{(2)\prime} = \overline{X}_{11} \int_0^{\overline{l}} \overline{N}^T \overline{N} d\xi, \overline{g}_e^{(0)\prime} = \overline{X}_{11} \lambda^2 \int_0^{\overline{l}} \overline{N}^T \frac{\partial^2 \overline{N}}{\partial \xi^2} d\xi - \overline{X}_{33} \eta^2 \int_0^{\overline{l}} \overline{N}^T \overline{N} d\xi \tag{A13}$$

References

[1] Liu, C., Ke, L.L., Wang, Y.S., Yang, J., Kitipornchai, S., Thermo-electro-mechanical vibration of piezoelectric nanoplates based on the nonlocal theory, *Composite Structures*, 106, 2013, 167-170.

[2] Ke, L.L., Wang, Y.S., Thermoelectric-mechanical vibration of piezoelectric nanobeams based on the nonlocal theory, *Smart Materials and Structures*, 21, 2012, 025018.

[3] Eringen, A.C., Theory of nonlocal plasticity, *International Journal of Engineering Science*, 21, 1983, 741-751.

[4] Eringen, A.C., Nonlocal continuum field theories, New York: Springer-Verlag; 2002.

[5] Zhang, D.P., Lei, Y., Wang, C.Y., Shen, Z.B., Vibration analysis of viscoelastic single-walled carbon nanotubes resting on a viscoelastic foundation, *Journal of Mechanical Science and Technology*, 31(1), 2017, 87-98.

[6] Wu, C.P., Lai, W.W., Free vibration of an embedded single-walled carbon nanotube with various boundary conditions using the RMVT-based nonlocal Timoshenko beam theory and DQ method, *Physica E*, 68, 2015, 8-21.

[7] Blasé, X., Rubio, A., Louie, S.G., Cohen, M.L., Stability and band gap constancy of boron nitride nanotubes, *Europhysics Letters*, 28, 1994, 335-341.

[8] Zenkour, A.M., Nonlocal transient thermal analysis of a single-layered graphene sheet embedded in viscoelastic medium, *Physica E*, 78, 2016, 87-97.

[9] Hache, F., Challamel, N., Elishakoff, I., Wang, C.M., Comparison of nonlocal continualization schemes for lattice beams and plates, *Archive of Applied Mechanics*, 87(7), 2017, 1105-1138.

[10] Lei, Y., Friswell, M.I., Adhikari, S., A Galerkin method for distributed systems with non-local damping, *International Journal of Solids and Structures*, 43, 2006, 3381-3400.

[11] Lei, Y., Finite element analysis of beams with nonlocal foundations, *47th AIAA/ASME/ASCE/AHS/ASC Structures, Structural Dynamics, and Materials Conferrence*, Newport, Rhode Island, 2006, 1-11.

[12] Zhao, X.C., Lei, Y., Zhou, J.P., Strain analysis of nonlocal viscoelastic Kelvin bar in tension, A*pplied Mathematics and Mechanics*, 29(1), 2008, 67-74.

[13] Friswell, M.I., Adhikari, S., Lei, Y., Non-local finite element analysis of damped beams, *International Journal of Solids and Structures*, 44, 2007, 7564-7576.

[14] Asemi, S.R., Farajpour, A., Thermo-electro-mechanical vibration of coupled piezoelectricnanoplate systems under non-

uniform voltage distribution embedded in Pasternak elastic medium, *Current Applied Physics*, 14, 2014, 814-832.
[15] Asemi, S.R., Farajpour, A., Asemi, H.R., Mohammadi, M., Influence of initial stress on the vibration of double-piezoelectric-nanoplate systems with various boundary conditions using DQM, *Physica E*, 63, 2014, 169-179.
[16] Kolahchi, R., Hosseini, H., Esmailpour, M., Differential cubature and quadrature-Bolotin methods for dynamic stability of embedded piezoelectric nanoplates based on visco-nonlocal-piezoelasticity theories, *Composite Structures*, 157, 2016, 174-186.
[17] Kolahchi, R., Zarei, M.S., Hajmohammad, M.H., Oskouei, A.N., Visco-nonlocal-refined Zigzag theories for dynamic buckling of laminated nanoplates using differential cubature-Bolotin methods, *Thin-Walled Structures*, 113, 2017, 162-169.
[18] Arefi, M., Zenkour, A.M., Size-dependent free vibration and dynamic analyses of piezo-electromagnetic sandwich nanoplates resting on viscoelastic foundation, *Physica B*, 521, 2017, 188-197.
[19] Bouafia, K., Kaci, A., Houari, M., Benzair, A., Tounsi, A., A nonlocal quasi-3D theory for bending and free flexural vibration behaviors of functionally graded nanobeams, *Smart Structures and Systems*, 19(2), 2017, 115-126.
[20] Bounouara, F., Benrahou, K.H., Belkorissat, I., Tounsi, A., A nonlocal zeroth-order shear deformation theory for free vibration of functionally graded nanoscale plates resting on elastic foundation, *Steel and Composite Structures*, 20(2), 2016, 227-249.
[21] Bellifa, H., Benrahou, K.H., Bousahla, A.A., Tounsi, A., Mahmoud, S.R., A nonlocal zeroth-order shear deformation theory for nonlinear postbuckling of nanobeams, *Structural Engineering and Mechanics*, 62(6), 2017, 695-702.
[22] Chaht, F.L., Kaci, A., Houari, M.S.A., Tounsi, A., Beg, O.A., Mahmoud, S.R., Bending and buckling analyses of functionally graded material (FGM) size-dependent nanoscale beams including the thickness stretching effect, *Steel and Composite Structures*, 18(2), 2015, 425-442.
[23] Besseghier, A., Houari, M.S.A., Tounsi, A., Mahmoud, S.R., Free vibration analysis of embedded nanosize FG plates using a new nonlocal trigonometric shear deformation theory, *Smart Structures and Systems*, 19(6), 2017, 601-614.
[24] Ahouel, M., Houari, M.S.A., Bedia, E.A.A., Tounsi, A., Size-dependent mechanical behavior of functionally graded trigonometric shear deformable nanobeams including neutral surface position concept, *Steel and Composite Structures*, 20(5), 2016, 963-981.
[25] Bedia, W.A., Benzair, A., Semmah, A., Tounsi, A., Mahmoud, S.R., On the thermal buckling characteristics of armchair single-walled carbon nanotube embedded in an elastic medium based on nonlocal continuum elasticity, *Brazilian Journal of Physics*, 45, 2015, 225-233.
[26] Belkorissat, I., Houari, M.S.A., Tounsi, A., Bedia, E.A.A., Mahmoud, S.R., On vibration properties of functionally graded nano-plate using a new nonlocal refined four variable model, *Steel and Composite Structures*, 18(4), 2015, 1063-1081.
[27] Zhou, Z., Wang, B., The scattering of harmonic elastic anti-plane shear waves by a Griffith crack in a piezoelectric material plane by using the non-local theory, *International Journal of Engineering Science*, 40, 2002, 303-317.
[28] Zhou, Z., Wu, L., Du, S., Non-local theory solution for a Mode I crack in piezoelectric materials, *European Journal of Mechanics A/Solids*, 25, 2006, 793-807.
[29] Quek, S.T., Wang, Q., On dispersion relations in piezoelectric coupled-plate structures, *Smart Materials and Structures*, 9, 2000, 859-867.
[30] Ke, L.L., Liu, C., Wang, Y.S., Free vibration of nonlocal piezoelectric nanoplates under various boundary conditions, *Physica E*, 66, 2015, 93-106.